Characterization of Photoinduced Isomerization and Back-Isomerization of the Cyanine Dye Cy5 by Fluorescence Correlation Spectroscopy

Jerker Widengren*,†,‡ and Petra Schwille§

Department of Spectroscopy and Photochemical Kinetics, and Department of Experimental Biophysics, Max-Planck Institute for Biophysical Chemistry, 370 77 Göttingen, Germany

Received: January 5, 2000; In Final Form: April 25, 2000

Cy5 is one of a few commercially available dyes in the near-infrared wavelength range. In this study, the fluorescence fluctuations of Cy5 have been investigated under steady-state excitation conditions by fluorescence correlation spectroscopy (FCS). The fluctuations in fluorescence are compatible with and can be used to characterize the photoinduced isomerization and back-isomerization, as well as the transitions between the singlet and triplet states of the dye. By employing a simple kinetic model, the rate constants of these processes can be determined. The model was used over a broad range of experimental conditions, where the influence on the isomerization properties of solvent viscosity, polarity, and temperature, excitation intensity and wavelength, and the presence of different side groups was investigated. We propose FCS as a useful and simple complementary approach to study isomerization processes of cyanine dyes yielding information about the rates of both the photoinduced isomerization and the back-isomerization, as well as of the kinetic properties of the triplet states. Our data show that for most excitation conditions relevant for ultrasensitive fluorescence spectroscopy a photostationary equilibrium is established between the isomeric forms, where approximately 50% of the Cy5 dye molecules can be expected to be in their weakly fluorescent cis states. The fluorophores therefore lose about half of their fluorescence capacity. This is of relevance for the performance of the dye in all applications of fluorescence spectroscopy where a high sensitivity or a fast readout is required, such as in single-molecule detection experiments and in many applications of confocal laser scanning microscopy.

1. Introduction

Cy5 is an activated carboxyl cyanine fluorophore that can be coupled with oligonucleotides, peptides and proteins.[1−3] Being one of a few commercially available fluorescent probes with an emission wavelength in the far-red spectral range, it has recently become a very important tool in ultrasensitive imaging and spectroscopy, especially for biological applications.[4−9] Cyanine dyes in general show a very strong $\pi \rightarrow \pi^*$ absorption, which can be tuned through the visible and the near-infrared region by variation of the length of the polymethinic chain joining the two heads of the cyanine dye.[10,11] In this way, they can be synthesized to absorb and emit at specific wavelength ranges. This makes them useful as donor and acceptor dyes in fluorescence resonance energy-transfer (FRET) experiments.[12] Cyanine dyes have also been used in applications of fluorescence spectroscopy and imaging where the simultaneous readout of two or several labels with different emission wavelengths is desired, as in experiments where colocalization or cross-correlation over time is performed.[13−15] For cell measurements, dyes excitable in the near-infrared (near-IR) range, such as Cy5 and Cy5.5, are preferable because a much lower autofluorescence and a higher transmittance through the cell media are to be expected in this wavelength range.[16−18]

The possibility to adapt the wavelength of emission and excitation, in combination with relatively high fluorescence quantum yields, high photostabilities, low pH sensitivities, and the possibility to use inexpensive laser diodes and highly efficient avalanche photodiodes in the near-IR range, has contributed to the frequent use of cyanine dyes in ultrasensitive fluorescence spectroscopy and fluorescence microscopy. For all applications of fluorescence spectroscopy, where a very high sensitivity or a high readout rate is required, as for detection of single molecules by fluorescence and applications of scanning confocal fluorescence microscopy, photophysical properties are of considerable importance. Originally, the interest in the photophysics of the cyanine dyes has been motivated from their widespread use as spectral sensitizers in photography,[19] as saturable absorbers for mode-locking and Q-quenching of lasers,[20,21] as initiators in photopolymerization,[19] as probes for the physical state and membrane potential of liposomes and synthetic bilayers,[22] and as potential sensitizers (merocyanines) for photodynamic therapy.[23−25] Consequently, much effort has been spent over the last decades to better understand the photophysical properties of these dyes.[26] Different transient[23,24,27−41] and photostationary[34,42−47] absorption spectroscopy techniques, as well as time-resolved[6,24,32,33,36,37,43,48−51] and photostationary[40,44,45,52,53] fluorescence measurements, laser-induced optoacoustic spectroscopy[44,45,54−56], nuclear magnetic resonance measurements,[24,49,57] and theoretical calculations[34,43,58−60] have been employed.

In ultrasensitive fluorescence spectroscopy, the overall performance of a dye is given by the total number and rate of fluorescence photons emitted per dye molecule, which are determined by the quantum yields of fluorescence and photodestruction, and by the turnover rates in the excitation−emission cycles. The turnover rates are limited by saturation as the excitation rates get comparable to the rates of deexcitation.

* Corresponding author. Fax: +49-551-2011006. Tel: +49-551-2011087. E-mail: jwideng@gwdg.de.
† Department of Spectroscopy and Photochemical Kinetics.
‡ Currently on leave from Department of Medical Biophysics, MBB, Karolinska Institutet 171 77 Stockholm, Sweden.
§ Department of Experimental Biophysics.

10.1021/jp000059s CCC: $19.00
Published on Web 06/17/2000

Generally, relaxation processes must be fast in order to effectively compete with fluorescence generation and internal conversion. On the other hand, for a saturating steady-state excitation, populations of photoinduced states with low quantum yields of formation have to be considered, such as triplet and photooxidized states. Such states can be significantly populated if their deactivation rates are of the same order as their rates of formation leading to a considerable decrease in the fluorescence emission rates. To determine the extent of population of additional transient states under such conditions, information is required not only about their quantum yields of formation but also about their deactivation rates.

Experimental and theoretical studies have shown that sterically nonhindered cyanine dyes in their monomeric forms generally exhibit low quantum yields of intersystem crossing and high quantum yields for trans−cis isomerization upon excitation.[27,29] However, in spite the many investigations that have been made on the isomerization properties of cyanine dyes, relatively few studies have revealed information about the photoinduced back-isomerization of photoisomerized cyanine dyes.[43−46,54,55] This fact probably reflects experimental difficulties of studying such deactivation processes by conventional spectroscopic techniques, such as flash photolysis, and with the methods applied, including steady-state fluorescence and laser-induced optoacoustic spectroscopy, a relative complicated sequence of operations are required in order to obtain the spectroscopic data.

In this study, the photophysical properties of Cy5 under steady-state excitation conditions are investigated by fluorescence correlation spectroscopy (FCS). FCS is a technique that derives information about dynamic processes on the molecular scale from the analysis of spontaneous fluctuations in fluorescence emission. It is shown that the fluorescence fluctuations of Cy5 are compatible with and can be used to characterize the photoinduced isomerization and back-isomerization, as well as the transitions between the singlet and triplet states of the dye. By employing a simple kinetic model, the rate constants of these processes can be determined. We conclude that FCS is a useful complementary approach to study isomerization processes of cyanine dyes yielding information about the rates of both the photoinduced isomerization and the back-isomerization, as well as of the kinetic properties of the triplet states.

2. Methods and Materials

In FCS, the fluctuating fluorescence emission arising from small quantities of fluorescent molecules is used to obtain information about dynamic processes on the molecular level.[61−64] These fluctuations are analyzed in the form of a normalized autocorrelation (AC) function:

$$G(\tau) = \frac{\langle I(t)\, I(t+\tau)\rangle}{\langle I\rangle^2} = \frac{\langle [\langle I\rangle + \delta I(t)][\langle I\rangle + \delta I(t+\tau)]\rangle}{\langle I\rangle^2} = 1 + \frac{\langle \delta I(t)\delta I(t+\tau)\rangle}{\langle I\rangle^2} \quad (1)$$

Here $I(t)$ signifies the detected fluorescence intensity, and $\delta I(t)$ denotes the fluctuations of $I(t)$ around its mean, $\langle I\rangle$. In principle, any dynamics, from the nanosecond to well over the millisecond time range, can be investigated as long as they manifest themselves as changes in the fluorescence intensity. In the early applications of the FCS technique, low detection efficiency combined with limited photostability of the fluorophores restricted the use of the method. By the introduction of a very small open detection volume (fractions of a femtoliter) in a confocal setup, and highly selective excitation and emission, a very high spatial and spectral discrimination has been reached. Beyond that, the use of silicon avalanche photodetectors with high detection quantum yields and low dark count levels and objectives with high numeric apertures has made it possible to increase signal-to-noise ratios considerably compared to early FCS experiments. Measurement times have been shortened drastically,[65] and it has become possible to perform measurements at the level of single molecules.[66−68]

The experimental setup used in this study has been described elsewhere and is based on the above principles.[65,69,70] The fluorescent samples are excited by a laser beam (Coherent Innova argon ion laser, 515 nm, Uniphase helium−neon laser, 632 nm, or Coherent Innova krypton ion laser, operated at 647 nm wavelength), which after reflection by a dichroic mirror (670DRLP02, Omega Optics (632 nm and 647 nm excitation), or 510DCLP AF Analysentechnik (515 nm excitation)) is focused by a microscope objective (Zeiss Plan-Neofluar 63× NA 1.2). The fluorescence is collected and then refocused by the same objective to the image plane, where a pinhole (radius 25 or 30 μm) is placed. The detection volume is defined by the dimensions of the focused laser beam (varying between 0.3 and 0.7 μm in beam waist radius) and the collection efficiency function of the confocal microscope.[69,70] A band-pass filter is used (690DF45, Omega Optics (for Cy5), or HQ575/70, AF Analysentechnik (for Cy3)) to discriminate fluorescence from laser light scattered at the excitation wavelength and from Raman scattered light of the solvent molecules. The fluorescence light is detected by two avalanche photodiodes (EG&G model SPCM-100), the output pulses of which are processed online by a PC-based correlator board with time resolution of 12.5 ns (ALV5000 with fast option, ALV).

Cy5 monoreactive dye, Cy5-dUTP, Cy5-dCTP, and Cy3 monoreactive dye were purchased from Pharmacia-Amersham, diluted in double-distilled water, ethanol, methanol, or ethylene glycol (spectroscopic purity) to nanomolar concentrations, and used without further purification. Cy5 (monoreactive dye) linked to a double-stranded M13 DNA, 24 base pairs long, and Cy5 linked to an IgG anti-mouse antibody (bisreactive dye) were obtained from Amersham. When dissolved in water, the Cy5 and Cy3 monoreactive dyes in their unlabeled form are believed to change into Cy5/Cy3-carboxylic acids, dropping the end group of the linker chain.[71]

3. Theoretical Background

Generally in fluorescence microscopy, the detected fluorescence is given as

$$I(t) = \int \mathrm{CEF}(\tilde{r})\, c(\tilde{r}, t) q k_{10} \Phi_f\, {}^1_1\mathrm{N}(\tilde{r},t)\, \mathrm{dV} \quad (2)$$

Here, $\mathrm{CEF}(\tilde{r})$ is the collection efficiency function of the confocal microscope setup, which is determined by the dimensions of the pinhole and the optical properties of the objective, $c(\tilde{r},t)$ denotes the concentration of fluorophores, and q accounts for the quantum efficiency of the detectors and the attenuation of the fluorescence in the passage from the sample volume to the detector areas. k_{10} is the deexcitation rate from the excited singlet state, Φ_f denotes the quantum yield of fluorescence, and ${}^1_1\mathrm{N}(\tilde{r},t)$ is the fraction of the fluorophores in the sample volume element that are in their excited singlet states. The product of the three latter parameters corresponds to the fluorescence emission rate per molecule.

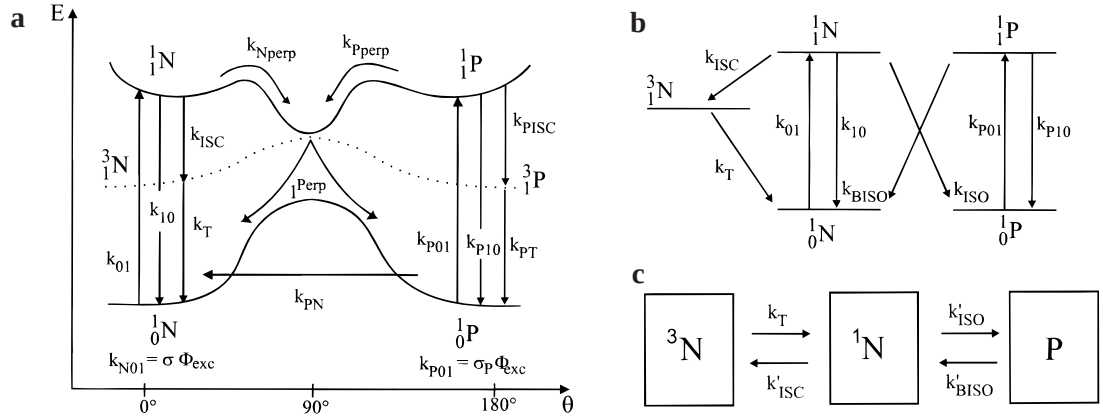

Figure 1. (a, left) Kinetic scheme normally adopted to model the photophysical behavior of carbocyanine dyes. In the model, $^1_0$N, $^1_1$N, and $^3_1$N denote the ground singlet, the first excited singlet, and triplet state of the thermodynamically stable conformation of the dye, which normally is the all-trans form. $^1_0$P, $^1_1$P, and $^3_1$P are the corresponding states of the photoisomerized form, which is usually in a mono-cis conformation. Upon isomerization the bond angle, denoted by Θ, in one of the double bonds of the conjugated hydrocarbon chain connecting the two headgroups of the dye is twisted by 180°. Photoinduced isomerization and back-isomerization take place from $^1_1$N and $^1_1$P via the partially twisted intermediate state, $_1$Perp. At $_1$Perp deactivation to the ground-state hypersurface takes place, either to $^1_0$N or to $^1_0$P. $k_{01} = \sigma\Phi_{exc}$, k_{ISC}, and k_T denote the excitation rate of $^1_0$N to $^1_1$N (where σ is the excitation cross section of $^1_0$N, and Φ_{exc} is the excitation intensity), intersystem crossing from $^1_1$N to $^3_1$N, and triplet-state decay from $^3_1$N to $^1_0$N. $k_{P01} = \sigma_P\Phi_{exc}$, k_{PISC}, and k_{PT} are the corresponding rate parameters for the photoisomerized state. k_{PN} is the rate of thermal deactivation of $^1_0$P to $^1_0$N in the absence of excitation. (b, top right) Simplified scheme of (a), where the partially twisted intermediate state, $_1$Perp, and the triplet state of the photoisomerized state, $^3_1$P, have been neglected. Photoinduced isomerization and back-isomerization are characterized by their overall effective rates, k_{ISO} and k_{BISO} (see eqs 11 and 12). Also, for the experimental conditions of our study the thermal back-isomerization from $^1_0$P to $^1_0$N, characterized by the rate parameter k_{PN} in (a), can be neglected (see text for further discussion). (c, bottom right) The three-state model used to characterize the fluorescence fluctuations observed in the FCS experiments presented in this study. Here ^{3}N, ^{1}N, and P correspond to the fractions of dye molecules that are in their trans-triplet ($^3_1$N), trans-singlet ($^1_0$N + $^1_1$N), and cis-singlet ($^1_0$P + $^1_1$P) states. Compared to (b), the transitions between the ground and excited states of ^{1}N and P have been neglected, since they typically take place on a time scale that cannot be resolved in the FCS measurements, and therefore only have to be considered as average distributions between the ground and excited-state dyes in N and P. k_{ISC}', k_{ISO}', and k_{BISO}' denote the effective rates of intersystem crossing from ^{1}N to ^{3}N, isomerization from ^{1}N to P, and back-isomerization from P to ^{1}N and are given by the corresponding rates, k_{ISC}, k_{ISO}, and k_{BISO} of (b), except for scaling factors corresponding to the fractions of dyes in the ^{1}N and P forms that are in their excited states (eqs 13−15).

If fluorescence fluctuations arise only from translational diffusion of the fluorescent molecules in and out of the sample volume element, the time-dependent part of the correlation function takes the following form:[65,69,72]

$$G_D(\tau) = \frac{1}{N_m}\left(\frac{1}{1 + 4D\tau/{\omega_1}^2}\right)\left(\frac{1}{1 + 4D\tau/{\omega_2}^2}\right)^{1/2} \qquad (3)$$

Here ω_1 and ω_2 are the distances from the center of the laser beam focus in the radial and axial direction, respectively, at which the collected fluorescence intensity has dropped by a factor of e^2 compared to its peak value. N_m is the mean number of fluorescent molecules within the effective volume of observation $\pi^{3/2}{\omega_1}^2\omega_2$ (sample volume element), and D is the diffusion coefficient of the fluorescent molecules. Equation 3 assumes the collected fluorescence profile to be Gaussian-shaped in the axial as well as in the radial direction. However, eq 3 can also provide a good approximation for a diffraction-limited distribution of the excitation intensity in the focal region of the laser beam when a matching confocal pinhole is used.[69] In FCS measurements, transient nonfluorescent states present themselves as fluorescence fluctuations superimposed on those caused by concentration changes due to translational motion of the fluorophores in and out of the sample volume element. These superimposed fluorescence fluctuations originate from changes in the excited singlet state population. Typically, the time range for formation and decay of many photoinduced transient states is much faster than those due to translational diffusion (the time scales can be further separated by variation of the sample volume element or the excitation intensity). Therefore, in the derivation of the fluorescence correlation function, one can in many cases treat fluctuations in fluorescence originating from changes in $^1_1$N($\tilde{r}$, t) separately from those due to changes in $c(\tilde{r},t)$.[70,73] But even for the case that the separation in time scale between the photophysical and diffusional events would not be so prominent, a separate treatment of the fluctuations of $^1_1$N($\tilde{r}$, t) and $c(\tilde{r}, t)$ is possible if diffusion properties are not changed significantly upon generation of a photoinduced transient state, as has also been shown for the case of chemical reactions.[74]

For conventional dyes previously investigated with FCS, such as fluoresceins and rhodamines, additional fluctuations in fluorescence are seen with increasing excitation intensities as the molecules enter and leave their triplet states. These fluctuations can be characterized by a simple three-level scheme (including the excited singlet, $^1_1$N, ground singlet, $^1_0$N, and lowest triplet, ^3N, states of Figure 1a,b) and can be expressed as functions of the kinetic rate constants for the transitions between the three states:[70,73]

$$G_T(\tau) = G_D(\tau)\left[1 + \frac{{}^3\bar{N}}{1 - {}^3\bar{N}}\exp(-\tau/\tau_T)\right] \qquad (4)$$

Here $G_D(\tau)$ is the time-dependent correlation function arising from number fluctuations due to translational diffusion, as given by eq 3. ${}^3\bar{N}$ is the mean fraction of fluorophores within the sample volume element that are in their triplet states, and τ_T is the relaxation time given by that eigenvalue of the kinetic scheme that is related to the triplet-state relaxation. Recently, FCS has also been used to investigate other photophysical processes, such as photoinduced electron transfer[75] and photoinduced transient states of different mutants of the green fluorescent protein.[76,77]

Photodegradation processes, although nonstationary in character, can also be characterized by FCS, if the time for translational diffusion through the detection volume is longer than the photochemical lifetime of the molecules under a given excitation.[78,79] This can occur owing to an increased size of the volume element, slower moving fluorescent molecules, very high excitation irradiances, or as a consequence of a low photostability of the dyes. Photodegradation then becomes evident in the experimental AC curves as a faster decay of the part of the curves related to translational diffusion:

$$G_T(\tau) = G_D(\tau)\left[1 + \frac{{}^3\bar{N}}{1 - {}^3\bar{N}}\exp(-\tau/\tau_T)\right] \times [1 - B + B\exp(-k_D\tau)] + 1 \quad (5)$$

Here an average effective photobleaching rate constant, k_D, within the sample volume element is assumed. The actual excitation intensity-dependent, and therefore space-dependent, homogeneous distribution of photobleaching rates within the sample volume element is regarded as an overall bleaching reaction related to the mean excitation intensity within the sample volume element involving a fraction B of all excited molecules. This assumption is reasonable considering that photobleaching is an irreversible process taking place on a time scale similar to that of translational diffusion, such that the dye molecules finally undergoing photobleaching will have experienced almost the whole range of excitation intensities within the sample volume element.

Kinetic Model for the Photodynamics of Cyanine Dyes. Most cyanine dyes that have no sterical constraints or substitutions in their polymethinic chains are believed to adopt an all-trans conformation in their ground states.[34,42] The major processes that occur following photoexcitation of a ground-state cyanine dye in its all-trans form, ${}^1_0\mathrm{N}$, to its first excited singlet state, ${}^1_1\mathrm{N}$, are given by[27,29]

$${}^1_1\mathrm{N} \xrightarrow{k_f} {}^1_0\mathrm{N} + h\nu \text{ (fluorescence)} \quad (6)$$

$${}^1_1\mathrm{N} \xrightarrow{k_{ISC}} {}^3_1\mathrm{N} \text{ (intersystem crossing to the lowest triplet state)} \quad (7)$$

$${}^1_1\mathrm{N} \xrightarrow{k_{IC}} {}^1_0\mathrm{N} \text{ (internal conversion)} \quad (8)$$

$${}^1_1\mathrm{N} \xrightarrow{k_{ISO}} {}^1_0\mathrm{P} \text{ (photoinduced trans}-\text{cis isomerization)} \quad (9)$$

The kinetic scheme of Figure 1a is normally adopted to account for the photophysical behavior of carbocyanine dyes.[36,40,43,48] The photoinduced isomerization is believed to involve a partially twisted intermediate excited state, ${}_1$Perp, which is deactivated very quickly by internal conversion to the ground-state hypersurface. After deactivation of ${}_1$Perp, branching takes place to either the ground state of the trans form, ${}^1_0\mathrm{N}$, or to that of the photoisomer, ${}^1_0\mathrm{P}$. The deactivation of ${}^1_1\mathrm{N}$ to ${}^1_0\mathrm{N}$ via ${}_1$Perp then contributes to the overall rate of internal conversion (eq 8), while the formation of ${}^1_0\mathrm{P}$ from ${}^1_1\mathrm{N}$ via ${}_1$Perp constitutes the effective rate of photoinduced trans−cis isomerization (eq 9). The photoisomer is believed to generally adopt a mono-cis conformation, formed after rotation around one of the double bonds in the polymethinic chain,[42] where Θ in Figure 1a denotes the rotation coordinate around the bond in question.

For most cyanine dyes in moderately viscous solvents at room temperature, the back-reaction of ${}^1_0\mathrm{P}$ to ${}^1_0\mathrm{N}$, denoted by k_{PN} in Figure 1a, is relatively slow, typically taking place in the millisecond time range.[27,31,36,38,40] A more efficient formation of all-trans isomers from ground-state photoisomers can be achieved by photoinduced back-isomerization. After excitation of the ground-state photoisomer, all-trans isomers in their ground states are formed in a similar fashion as for the photoinduced trans−cis isomerization, k_{ISO}, via branching over ${}_1$Perp.

Triplet-state formation in cyanine dyes has been found to be relatively inefficient, with quantum yields of formation of the order 10^{-3} after excitation, and for most cyanine dyes the lowest triplet state is not believed to be involved in the isomerization process, which is thought to entirely be generated via the excited singlet state.[27−29,37,41]

The Modified Correlation Function. Under most conditions relevant for FCS, the transitions contained in Figures 1a−c (except for the ground-state thermal back-isomerization, k_{PN}) can be assumed to take place on a time scale that is much faster than the molecular observation time determined by translational diffusion of the fluorescent molecules in and out of the sample volume element. Furthermore, isomerization and triplet-state formation are not believed to change the diffusion properties of the Cy5 fluorophores drastically. Consequently, in the derivation of the fluorescence AC function the fluctuations in fluorescence generated by the transitions given in Figure 1a, denoted by δI_{fast}, can be treated separately from those due to translational diffusion, denoted by δI_D

$$G(\tau) = \langle I(t)\, I(t+\tau)\rangle/\langle I\rangle^2 = \langle[\langle I\rangle + \delta I_D(t) + \delta I_{fast}(t)] \times [\langle I\rangle + \delta I_D(t+\tau) + \delta I_{fast}(t+\tau)]\rangle/\langle I\rangle^2 = [\langle \delta I_D(t)\delta I_D(t+\tau)\rangle + \langle \delta I_{fast}(t)\delta I_{fast}(t+\tau)\rangle]/\langle I\rangle^2 + 1 = G_D(\tau) + G_{fast}(\tau) + 1 \quad (10)$$

where $G_{fast}(\tau)$ denotes the part of the correlation function originating from the photophysically generated fluctuations in fluorescence, as given by Figure 1a.

To simplify the kinetic treatment of the kinetic scheme given in Figure 1a, we disregard the partially twisted intermediate state, ${}_1$Perp. This state is typically deactivated in the picosecond to nanosecond time scale to either ${}^1_0\mathrm{P}$ or ${}^1_0\mathrm{N}$.[27] Moreover, most cis isomers of thiacarbocyanine dyes are believed not to fluoresce at room temperature and are upon excitation mainly deactivated through internal conversion.[27,43,44,46,54] In the further treatment, we therefore regard the fluorescence capacity of the photoisomer as negligible. With a very fast deactivation channel through internal conversion, the quantum yield of triplet-state formation from ${}^1_1\mathrm{P}$ is likely to be very low. In addition, experimental[36,37] and theoretical[59] studies indicate that there is a considerable activation energy barrier for transitions between the triplet states of the trans and the cis forms over the perpendicular form. This limits the formation of molecules in the ${}^3_1\mathrm{P}$ state formed via ${}^3_1\mathrm{N}$. Consequently, the population of ${}^3_1\mathrm{P}$ is likely to be very small and will not be further taken into consideration.

Given the above assumptions, the kinetic schedule of Figure 1a can be simplified to that of Figure 1b, where k_{ISO} and k_{BISO} denote the effective rates of photoinduced isomerization and back-isomerization and are given by

$$k_{ISO} = \frac{\Phi_{ISO}}{1 - \Phi_{ISO}}[k_{10} + k_{ISC}] \quad (11)$$

$$k_{BISO} = \frac{\Phi_{BISO}}{1 - \Phi_{BISO}}[k_{P10}] \quad (12)$$

where Φ_{ISO} and Φ_{BISO} are the effective yields of photoinduced isomerization and back-isomerization from the $^1_1$N and from the $^1_1$P state, respectively. In this study, the time resolution of the FCS measurements is limited by the fastest channel of the PC-based correlator to 12.5 ns. However, the transitions between the singlet states, within each of the isomerization forms, i.e., between $^1_0$N and $^1_1$N and between $^1_0$P and $^1_1$P, respectively, take place in the nanosecond time scale. These transitions will therefore in general not be resolved on the time scale of the FCS measurements, where the other dynamic processes related to intersystem crossing or trans−cis isomerization were found to take place.

Considering that the decay rates, k_{10} and k_{P10}, of the excited states, $^1_1$N and $^1_1$P, to their ground states, $^1_0$N and $^1_0$P, can be expected to be much faster than any of the rates related to trans−cis isomerization or to singlet−triplet transitions, the kinetic scheme of Figure 1b can be further reduced to that of Figure 1c, containing the fluorescent singlet form ^{1}N ($^1_0$N and $^1_1$N), the nonfluorescent isomerized form P ($^1_0$P and $^1_1$P), and the nonfluorescent triplet state ^{3}N. In Figure 1c, the effective transition rates from ^{1}N and P will be the same as those from the excited-state levels of ^{1}N and P, except for scaling factors corresponding to the fractions of singlet-state dyes in the ^{1}N and P forms that are in their excited states:

$$k_{ISC}' = \frac{k_{01}}{k_{10} + k_{01}} k_{ISC} = \frac{\sigma\Phi_{exc}}{k_{10} + \sigma\Phi_{exc}} k_{ISC} \tag{13}$$

$$k_{ISO}' = \frac{k_{01}}{k_{10} + k_{01}} k_{ISO} = \frac{\sigma\Phi_{exc}}{k_{10} + \sigma\Phi_{exc}} k_{ISO} \tag{14}$$

$$k_{BISO}' = \frac{k_{P01}}{k_{P10} + k_{P01}} k_{BISO} = \frac{\sigma_P\Phi_{exc}}{k_{P10} + \sigma_P\Phi_{exc}} k_{BISO} = \{k_{P10} \gg \sigma_P\Phi_{exc}\} = \sigma_{BISO}\Phi_{exc} \tag{15}$$

Here σ and σ_P are the excitation cross sections of the ground singlet states of $^1_0$N and $^1_0$P. Φ_{exc} denotes the mean excitation intensity within the detection volume. k_{10} and k_{P10} are the rates of deactivation of the singlet excited states $^1_1$N and $^1_1$P to their respective singlet ground states, k_{ISC} is the intersystem-crossing rate from $^1_1$N to the triplet state, $^3_1$N (see Figure 1a,b). $\sigma_{BISO} = \sigma_P k_{BISO}/k_{P10}$ denotes the effective cross section for back-isomerization of the cis state.

In the following treatment of the photophysically generated fluctuations, we assume for simplicity that the excitation intensity is uniform over the sample volume element. In order to find the expression for $G_{fast}(t)$, the following system of coupled first-order linear differential equations can be established according to the simplified kinetic scheme of Figure 1c

$$\frac{d}{dt}\begin{pmatrix} {}^1N(t) \\ {}^3N(t) \\ P(t) \end{pmatrix} = \begin{bmatrix} -(k_{ISC}' + k_{ISO}') & k_T & k_{BISO}' \\ k_{ISC}' & -k_T & 0 \\ k_{ISO}' & 0 & -k_{BISO}' \end{bmatrix} \begin{pmatrix} {}^1N(t) \\ {}^3N(t) \\ P(t) \end{pmatrix} \tag{16}$$

where k_T denotes the triplet-state deactivation rate to the ground singlet state, $^1_0$N. The correlation function expresses the probability of a photon emission at a time τ given a photon emission at time 0. For a fluorophore at a fixed position being subject to a constant excitation intensity, this probability will be proportional to $^1N(\tau)$, which is obtained from the solution of eq 16 with the following boundary condition:

$$\begin{pmatrix} {}^1N(0) \\ {}^3N(0) \\ P(0) \end{pmatrix} = \begin{pmatrix} 1 \\ 0 \\ 0 \end{pmatrix} \tag{17}$$

This condition follows from the assumption that only the ^{1}N state is fluorescent and, when a fluorescence photon has been emitted, the fluorophore consequently has to be in the ground singlet state of N. The general solution of eq 16, given the boundary condition of eq 17, can be expressed as

$$\begin{pmatrix} {}^1N(\tau) \\ {}^3N(\tau) \\ P(\tau) \end{pmatrix} = \sum_{i=1}^{3} \begin{bmatrix} A_i\nu_i(1)e^{\lambda_i\tau} \\ A_i\nu_i(2)e^{\lambda_i\tau} \\ A_i\nu_i(3)e^{\lambda_i\tau} \end{bmatrix} \tag{18}$$

where $\bar{\nu}_i = (\nu_i(1), \nu_i(2), \nu_i(3))$ denotes the ith eigenvector, λ_i is the ith eigenvalue of the differential equation matrix above, and A_i is a scaling factor to the ith eigenvector given by the boundary condition of eq 17. The eigenvalues are given by

$$\lambda_1 = 0$$

$$\lambda_{2,3} = -[[k_{ISC}' + k_T + k_{ISO}' + k_{BISO}']/2 \pm ([k_{ISC}' + k_T + k_{ISO}' + k_{BISO}']^2/4 - k_{ISO}'k_T - k_{ISC}'k_{BISO}' - k_Tk_{BISO}')^{1/2}] \tag{19}$$

The first eigenvalue, λ_1, is equal to zero, and the first component of the corresponding eigenvector scaled with A_1, $A_1\nu_1(1)$, represents the steady-state concentration of ^{1}N, denoted by $^1\bar{N}$. The multiplicative factors to the exponential terms of $^1N(\tau)$, as contained in eq 18, are given by

$$A_1\nu_1(1) = \frac{k_Tk_{BISO}'}{\alpha} = {}^1\bar{N} \tag{20a}$$

$$A_2\nu_2(1) = (\beta + \gamma)(k_T\gamma + \delta)/(4\alpha\gamma) \tag{20b}$$

$$A_3\nu_3(1) = (\beta - \gamma)(k_T\gamma - \delta)/(4\alpha\gamma) \tag{20c}$$

where

$$\alpha = k_{ISO}'k_T + k_{ISC}'k_{BISO}' + k_Tk_{BISO}'$$

$$\beta = k_{ISC}' + k_{ISO}' + k_T - k_{BISO}'$$

$$\gamma = ((k_{ISC}' + k_{ISO}')^2 + (k_{BISO}' - k_T)^2 + 2(k_{ISO}' - k_{ISC}')(k_{BISO}' - k_T))^{1/2}$$

$$\delta = k_T(k_{ISO}' + k_{BISO}' - k_T - k_{ISC}') + 2k_{ISC}'k_{BISO}'$$

For a fluorophore under stationary excitation intensity, the normalized correlation function for the photophysically generated fluctuations in fluorescence can be expressed as

$$G_{fast}(t) = \frac{\langle \delta I_{fast}(t)\, \delta I_{fast}(t+\tau)\rangle}{\langle I\rangle^2} = \frac{(k_{10}q\Phi_f\, {}^1_1\bar{N})(k_{10}q\Phi_f)({}^1_1N(\tau) - {}^1_1\bar{N})}{(k_{10}q\Phi_f\, {}^1_1\bar{N})^2} \tag{21}$$

where q and Φ_f are defined in connection with eq 2. At time scales well above nanoseconds, and in analogy to eqs 13 and 14, the steady-state as well as the time-dependent population of the excited singlet state of the all-trans form, denoted by

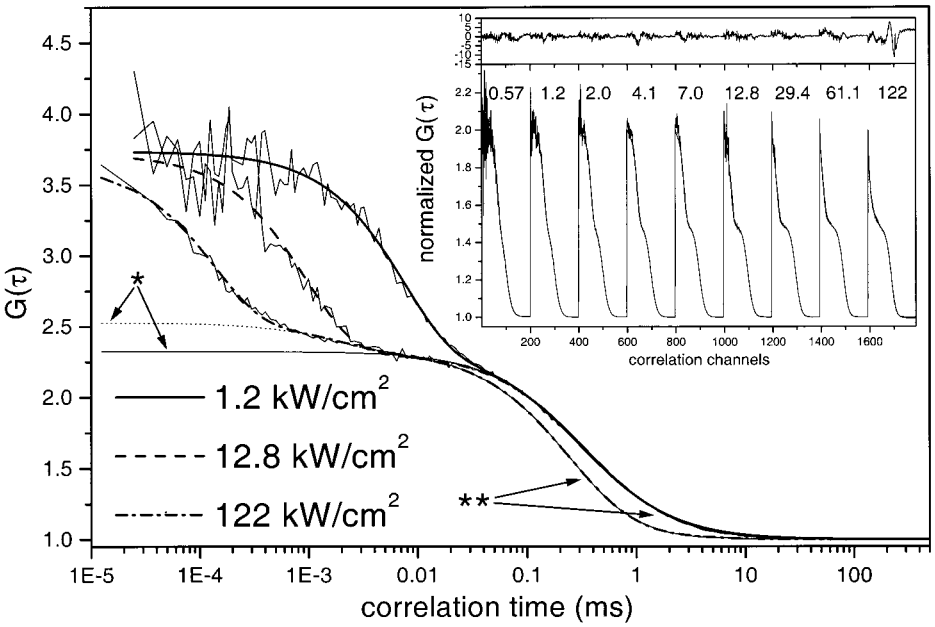

Figure 2. FCS curves of Cy5 in aqueous solution measured under 1.2, 12.8, and 122 kW/cm^2 excitation (647 nm excitation wavelength). A major relaxation process with a relative amplitude of about 50% is observed, whose amplitude did not change significantly with excitation intensity. The relaxation times of this exponential process, which can be mainly attributed to trans−cis isomerization, were however drastically reduced with higher excitation intensities. For excitation intensities above approximately 50 kW/cm^2, triplet-state population can be observed as an additional relaxation process (*). In Figure 2, the amplitude of this process was found to be approximately 10% at 122 kW/cm^2 (thin dotted curve indicates the shape of the FCS curves in the absence of the first relaxation process), while at 1.2 and 12.8 kW/cm^2 no second relaxation process due to population of triplet states could be observed (thin solid line). At excitation intensities exceeding 100 kW/cm^2, a faster overall decay of the FCS curves can be observed (**), which is due to photobleaching of the dye molecules during their transit through the sample volume element. (To better visualize the differences, all correlation curves have been normalized with respect to each other corresponding to the case that they would originate from an equal average number of molecules in the sample volume element.) Inset: Global analysis of nine correlation curves of Cy5 in aqueous solution that were measured at 647 nm excitation with excitation intensities ranging from 0.57 to 122 kW/cm^2 (excitation intensities in kW/cm^2 are indicated above each individual curve).

${}_1^1\bar{N}$ and ${}_1^1N(\tau)$, have a fixed relation to ${}^1\bar{N}$ and ${}^1N(\tau)$, respectively, which is given by $k_{01}/(k_{01} + k_{10})$:

$$ {}_1^1\bar{N} = A_1\nu_1(1)k_{N01}/(k_{N01} + k_{N10}) \qquad (22a) $$

$$ {}_1^1N(\tau) = {}^1\mathrm{N}(\tau)\frac{\mathrm{k}_{01}}{\mathrm{k}_{01} + \mathrm{k}_{10}} = [A_1\nu_1(1) + A_2\nu_2(1)\mathrm{e}^{\lambda_2\tau} + A_3\nu_3(1)\mathrm{e}^{\lambda_3\tau}]k_{01}/(k_{01} + k_{10}) \qquad (22b) $$

$G_{fast}(\tau)$ can then be rewritten as

$$ G_{fast}(\tau) = \frac{(k_{10}q\Phi_f{}^1\bar{N})(k_{10}q\Phi_f)({}^1N(\tau) - {}^1\bar{N})}{(k_{10}q\Phi_f{}^1\bar{N})^2} = \frac{{}^1N(\tau) - {}^1\bar{N}}{{}^1\bar{N}} = \frac{A_2\nu_2(1)\mathrm{e}^{\lambda_2\tau} + A_3\nu_3(1)\mathrm{e}^{\lambda_3\tau}}{A_1\nu_1(1)} \qquad (23) $$

For the full correlation function, using $1/\lambda_2$, $1/\lambda_3 \ll \tau_D \approx \omega_1{}^2/4D$, one will arrive at

$$ G(\tau) = \frac{1}{N_m}\left(\frac{1}{1 + 4D\tau/\omega_1{}^2}\right)\left(\frac{1}{1 + 4D\tau/\omega_2{}^2}\right)^{1/2}[1 + G_{fast}(\tau)] + 1 = \frac{1}{N_m{}^1\bar{N}}\left(\frac{1}{1 + 4D\tau/\omega_1{}^2}\right)\left(\frac{1}{1 + 4D\tau/\omega_2{}^2}\right)^{1/2}{}^1\mathrm{N}(\tau) + 1 = \frac{1}{N_mA_1\nu_1(1)}\left(\frac{1}{1 + 4D\tau/\omega_1{}^2}\right)\left(\frac{1}{1 + 4D\tau/\omega_2{}^2}\right)^{1/2} \times [A_1\nu_1(1) + A_2\nu_2(1)\mathrm{e}^{\lambda_2\tau} + A_3\nu_3(1)\mathrm{e}^{\lambda_3\tau}] + 1 \qquad (24) $$

4. Results and Discussion

Excitation Dependence in Aqueous Solution. Cy5 monofunctional dye was dissolved in water to concentrations in the nanomolar range and excited at 515 nm (argon ion laser), 632 nm (helium−neon laser), and 647 nm (krypton ion laser) in the FCS setup described above. In addition to the relaxation process due to translational diffusion as given by eq 3, the measured FCS curves revealed a major relaxation process, which could be fitted as an additional exponential process (Figure 2), with relative amplitudes of about 50% of the total amplitudes of the FCS curves. Upon variation of the excitation intensity, the relative amplitude of the relaxation process did not change significantly, except for excitation intensities close to or above saturation, where a slight drop of the relaxation amplitude could be noticed. The inverse relaxation time (the relaxation rate) of this exponential process, on the other hand, showed a linear dependence to the applied excitation intensity. When exciting at 647 nm, a second exponential process could be observed at excitation intensities of about 50 kW/cm^2 and higher (100 kW/cm^2 and higher at 632 nm excitation), which had a considerably lower relative amplitude. The amplitude of this second process increased slightly with the applied excitation intensity (Figure 2). The observed dependence on excitation intensity of the two exponential relaxation processes in the FCS curves is compatible with formation of transient dark states by photoinduced isomerization and intersystem crossing, as described above. Assuming the models of Figure 1a−c, a global fitting analysis was introduced. In this analysis, 5−10 different correlation curves were recorded under identical conditions, except that the excitation intensities were varied, and were then fitted simultaneously (inset, Figure 2, shows a global fit of 9 curves of

Cy5 measured in aqueous solution). In the fitting procedure, the intensity-independent photophysical parameters, k_{10}, σ, σ_{BISO}, k_{ISO}, k_{ISC}, and k_T were kept in common for all measured curves. These parameters determine the amplitudes and relaxation times of the exponential processes in the FCS curves, as given by eqs 13−15, 19, 20, and 24. On the other hand, the diffusional properties, given by the parameters $\tau_D = \omega_1^2/4D$ and ω_2/ω_1, were allowed to vary individually for each curve in order to minimize the influence of them on the determination of the photophysical parameters. The fluorescence lifetime of Cy5 has been reported to be 1.0 and 1.4 ns for the free dye[80] and Cy5-dCTP[81] in aqueous solution. These values were used to fix the fluorescence decay rates, k_{10}, of Cy5 (1.0 ns) and the Cy5-labeled molecules (1.4 ns), since otherwise a too strong covariance was found between k_{10} and σ, making it impossible to fit the two parameters simultaneously. The measured FCS curves showed a good correspondence to the model given by Figure 1c, and the resulting parameter values from the global fits were reproducible from one set of correlation curves to another.

In Figure 3 the relaxation rates and amplitudes calculated from the parameters obtained from the global fit (lines and crosses) are compared to the rates and amplitudes obtained when the correlation curves were fitted individually (squares). One can note that the two fast relaxation terms of the AC functions, as given by eq 24, can only be assigned to specific processes if the time range for the transitions to and from the different states are well separated. For excitation intensities below 1 kW/cm^2 (at 647 nm excitation), where trans−cis isomerization takes place at a slower time scale than singlet−triplet transitions, the relative fraction of isomerized states and the relaxation rate for the transitions to and from P are given by $A_3\nu_3(1)$ and λ_3. In contrast, above 10 kW/cm^2 the isomerization is much faster than the singlet−triplet transitions and is then represented by $A_2\nu_2(1)$ and λ_2. (The relative triplet-state population and the transitions to and from the triplet state are then consequently characterized by $A_2\nu_2(1)$ and λ_2 below 1 kW/cm^2 and by $A_3\nu_3(1)$ and λ_3 above 10 kW/cm^2). In the intermediate intensity range, between 1 and 10 kW/cm^2, where the relaxation times of the two terms are similar, the fast part of the correlation curves, $G_{fast}(\tau)$, will consist of two exponential terms of about equal amplitude, although the population of the triplet states of the Cy5 molecules will be negligible. At excitation intensities above 20 kW/cm^2, where fluorescence saturation is present and triplet-state formation can be observed, the relative population of isomerized fluorophores is decreased. A decrease in the isomerized fraction of the fluorophores is to be expected from the assumption that k_{P10} is very fast, since in an excitation intensity range where fluorescence saturation is present k_{BISO}' can still be expected to increase linearly to the excitation intensity, while k_{ISO}' is approaching an asymptotic level (equal to k_{ISO}), as can be seen from eqs 14 and 15.

Except for variations in excitation efficiencies, no major changes in the isomerization, nor in the triplet-state properties could be observed with variation of the excitation wavelength. The relative population of the fluorophores in the isomerized form measured at excitation intensities in the lower range, and given by the relaxation amplitude of $A_3\nu_3(1)$, was found to decrease with shorter excitation wavelengths. Compared to excitation at 647 nm, where $A_3\nu_3(1)$ was about 0.52 at lower excitation intensities, the relative amplitudes dropped to about 0.46 and 0.38 at 632 and 515 nm excitation, respectively (Figure 4). This indicates that the effective rate of isomerization decreases relatively more than that of back-isomerization when

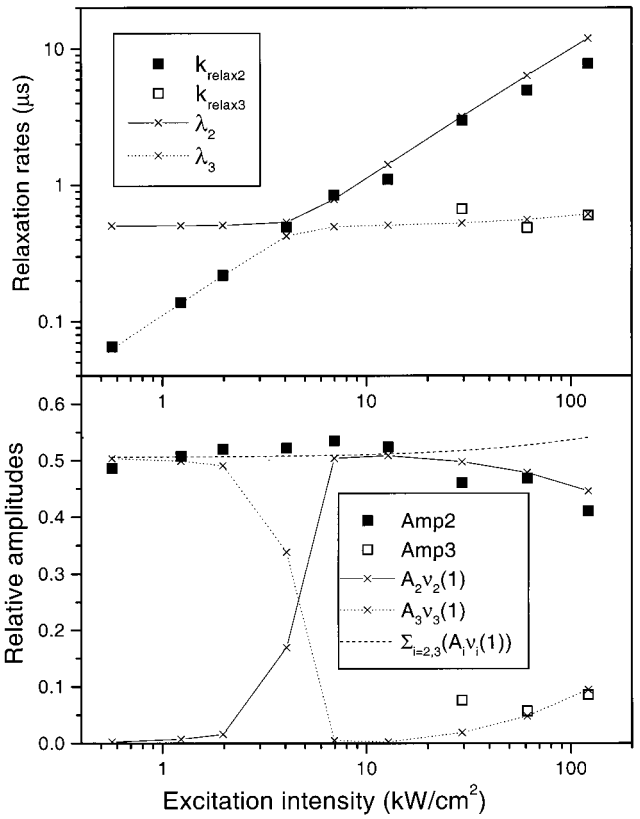

Figure 3. Relaxation rates and amplitudes, which are calculated from the parameters obtained from the global fit shown in the inset of Figure 2 (lines with crosses), compared to those obtained when the correlation curves were fitted individually (squares). One can note that the relaxation rates and amplitudes, as given by eq 24, do not represent the same process over the whole excitation intensity range. For excitation intensities below 1 kW/cm^2 (at 647 nm excitation), the relative fraction of isomerized states and the relaxation rate for the transitions to and from P are given by $A_3\nu_3(1)$ and λ_3, and above 10 kW/cm^2 they are given by $A_2\nu_2(1)$ and λ_2. The relative triplet-state population and the transitions to and from the triplet state are then consequently characterized by $A_2\nu_2(1)$ and λ_2 below 1 kW/cm^2 and by $A_3\nu_3(1)$ and λ_3 above 10 kW/cm^2. In the intermediate intensity range, between 1 and 10 kW/cm^2, where the relaxation times of the two terms are similar, the fast part of the correlation curves, $G_{fast}(\tau)$, will consist of two exponential terms of about equal amplitude, although the population of the triplet states of the Cy5 molecules will be negligible. At excitation intensities above 20 kW/cm^2, where fluorescence saturation is present and triplet-state formation can be observed, the relative population of isomerized fluorophores is decreased. This decrease can be attributed to saturation of the $^1_1$N state (while the $^1_1$P state, on the other hand, is assumed not to be saturated owing to a very fast rate of deactivation to $^1_0$P).

going from excitation at 647 nm to 632 or 515 nm excitation. The deactivation of the excited states of the N and P forms should not be affected by the history of excitation, such that the quantum yields of isomerization and back-isomerization would change with the excitation wavelength. Instead, this decrease in the relative population of the isomerized state with shorter excitation wavelengths implies that the ratio of the excitation cross section of the photoisomer, σ_P, to that of the all-trans form, σ, is increased. However, from the relatively small change in amplitudes of the isomerization relaxation process one can conclude that the excitation spectra of the two forms differ only to a limited extent. This is in line with what has been found experimentally[26,28,42,44] and theoretically[34] for other cyanine dyes.

At excitation intensities above 100 kW/cm^2 (647 nm excitation), a distinctly faster overall decay of the AC curves due to

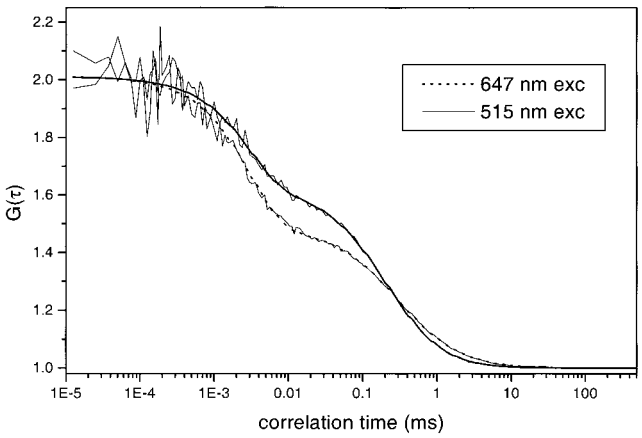

Figure 4. Two correlation curves of Cy5 in aqueous solution excited at 647 nm (solid line) and at 515 nm (dashed line) with similar rates of excitation (excitation intensities of 3.3 and 260 kW/cm^2, respectively). A significant difference in the amplitude of the isomerization process could be noticed, 0.52 (at 647 nm excitation), compared to 0.38 (at 515 nm excitation), indicative of a relatively higher excitation cross section of the cis form compared to that of the trans configuration at excitation wavelengths below 647 nm.

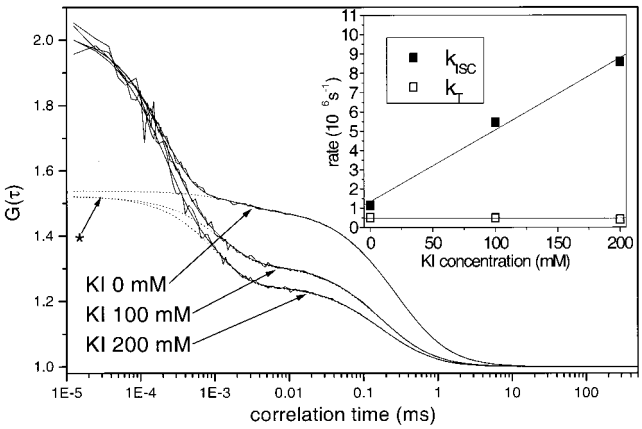

Figure 5. Effect of addition of potassium iodide (FCS curves measured at 0, 100, and 200 mM concentration of KI in an aqueous solution, excitation at 647 nm with 50 kW/cm^2). The dashed curves show the shape of the FCS curves in the absence of the first relaxation process, showing the contribution of singlet−triplet interactions. A noticeable increase of the triplet-state population could be observed upon addition of KI. From global analysis, where correlation curves for a certain KI concentration were measured at different excitation intensities and fitted simultaneously, the intersystem-crossing rate, k_{ISC}, was found to increase linearly with the KI concentration (inset), while the other photophysical parameters were not affected by the concentration of KI.

photodegradation could be noticed (see Figure 2). The AC curves recorded in the presence of photobleaching were fitted to eq 5. From the experimentally determined rates of photodegradation, and from the calculated population of the excited singlet state of the trans form at the excitation intensity used, given the photophysical parameters determined above, the quantum yield of photobleaching could be estimated to be 2×10^{-5}. This is a slightly higher yield of photobleaching than what has been found from FCS measurements for rhodamine dyes at similar excitation rates, but significantly lower than those of many other dyes, such as fluoresceins.[78,79,82] For rhodamines and fluoresceins, the yield of photobleaching increases with higher excitation intensities. This can be attributed to excitation to higher excited states, which have considerably lower photostabilities owing to photoionization. Similarly, the quantum yield of photobleaching of Cy5 can be expected to be much higher at excitation intensities in the range of saturation. Indeed, in cuvette experiments, at excitation intensities far below the saturation range, the photobleaching quantum yield of Cy5 has been determined to be 5×10^{-6}.[82]

Although the fluorescence fluctuations observed via the FCS curves are compatible with the kinetic scheme of Figure 3, FCS measurements cannot in general offer an identification of the transient states involved. In order to further test the origin of the fluctuations, and to investigate the environmental dependence of the photophysical properties of Cy5, additional FCS measurements were undertaken under different environmental conditions.

Addition of Potassium Iodide. Potassium iodide is known to enhance the rate of intersystem crossing of many dyes owing to the so-called heavy-atom effect,[83] and addition of potassium iodide has previously been observed to generate a dramatic increase of the population of the triplet states of rhodamine 6G observed in FCS measurements.[70] To investigate the identity of the second low-amplitude exponential process, which showed photodynamic features identical to those of triplet-state formation, potassium iodide was added in 100 and 200 mM concentrations to an aqueous solution of Cy5. FCS curves were recorded under different excitation intensities and subsequently fitted globally, as described above (Figure 5). From the individual FCS curves an evident increase in the amplitude of the second exponential could be observed with increasing concentrations of potassium iodide. The resulting parameters from the global fits are given in Table 1. No significant change in the parameters could be observed except for the intersystem-crossing rate, which increased linearly with the concentration of potassium iodide (inset, Figure 5). These findings support the assumption that the second exponential observed in the FCS curves is generated from singlet−triplet transitions. We could not observe any effect of addition of potassium iodide on the isomerization kinetics, which is in contrast to the findings in an early study,[47] where an increased isomerization rate was observed upon addition of potassium iodide. However, our results are in agreement with other previous reports, based mainly on time-resolved fluorescence studies, which state that the triplet state of most cyanine dyes is not involved in major conformational changes, but rather prevents or limits isomerization, and therefore is believed to be a competitive process to trans−cis isomerization.[28−30] The quenching constant of iodide for the transition from $^1_1$N to $^3_1$N was calculated to be 4×10^7 M^{-1} s^{-1}, which is 2 orders of magnitude lower than that found for rhodamine6G (Rh6G) in water. This big difference cannot be explained from the somewhat lower diffusion coefficient of Cy5 to that of Rh6G (estimated in our FCS measurements to be 2.5×10^{-10} m^2/s for Cy5 and 2.8×10^{-10} m^2/s for Rh6G) and indicates that steric and charge effects as well as differences in energies between the electronic states are also of importance for the overall quenching efficiency.

Solvent Dependence. FCS curves of Cy5 were measured at different excitation intensities in methanol, ethanol, propanol, and ethylene glycol and were subsequently fitted globally. From the obtained photophysical parameters (Table 1), one can observe that the isomerization parameters differ significantly from one solvent to another. To identify the major solvent parameters determining the isomerization kinetics, sucrose and sodium chloride were added separately to an aqueous solution of Cy5 to change the viscosity and polarity of the solvent, respectively. While addition of sucrose significantly slowed the isomerization kinetics and the diffusion time (Figure 6), no effect was observed by addition of 0.5 M sodium chloride. This suggests that the observed differences in the isomerization parameters between the solvents can mainly be attributed to different viscosities rather than to differences in polarity. This

TABLE 1: Photophysical Parameters of Cy5 under Various Conditions Obtained from Global Analysis of FCS Curves Measured under Different Excitation Intensities[a]

probe	solvent	viscosity (cP)	λ_{exc} (nm)	σ (10^{-16} cm^2) ±30%	σ_{BISO} (10^{-16} cm^2) ±30%	k_{ISO} (10^6 s^{-1}) ±30%	k_{ISC} (10^6 s^{-1}) ±50%	k_T (10^6 s^{-1}) ±50%
Cy5	water	1.0	632	4.3	0.13	25	1.1	0.5
Cy5	water + sucrose 30%	3.2	632	4.5	0.087	14	1.1	0.3
Cy5	water + sucrose 40%	6.2	632	4.7	0.059	8.0	0.6	0.24
Cy5	water + 0.5 M NaCl		632	4.6	0.13	26	1.1	0.3
Cy5	EtOH	1.2	632	3.6	0.13	30.5	3.8	0.74
Cy5	MeOH	0.6	632	3.2	0.14	51	6.0	3.2
Cy5	ethylene glycol	19.9	632	4.4	0.042	5.5	0.5	0.1
Cy5	PrOH	2.3	632	4.1	0.092	16	1.8	0.3
Cy5−dUTP	water	1.0	632	4.3	0.082	12.4	0.85	0.3
Cy5−dCTP	water	1.0	632	3.6	0.093	11.6	0.75	0.47
Cy5−DNA	water	1.0	632	4.1	0.041	5.7	0.43	0.11
Cy5−IgG	water	1.0	632	4.3 (fixed)	0.043	1.5	0.4	0.16
Cy5	water	1.0	647	8.1	0.17	21	0.83	0.50
Cy5	water + 100 mM KI		647	8.5	0.15	21	5.5	0.49
Cy5	water + 200 mM KI		647	8.4	0.17	23	8.6	0.42
Cy5	water	1.0	515	0.085	0.0026	19	1.0 (fixed)	0.5 (fixed)
Cy3	water	1.0	515	1.3	0.095	69	1.0 (fixed)	0.5 (fixed)

[a] σ is the excitation cross section of $^1_0$N, and $\sigma_{BISO} = \sigma_P k_{BISO}/k_{P10}$ is the effective excitation cross section for back-isomerization from $^1_0$P, where k_{BISO} is the back-isomerization rate from $^1_1$P, given by eq 12, k_{P10} is the deactivation rate of $^1_1$P to $^1_0$P, and σ_P is the excitation cross section of $^1_0$P. k_{ISO} is the isomerization rate from $^1_1$N, given by eq 11, k_{ISC} is the rate of intersystem crossing from $^1_1$N to $^3_1$N, and k_T is the triplet-state deactivation rate from $^3_1$N to $^1_0$N.

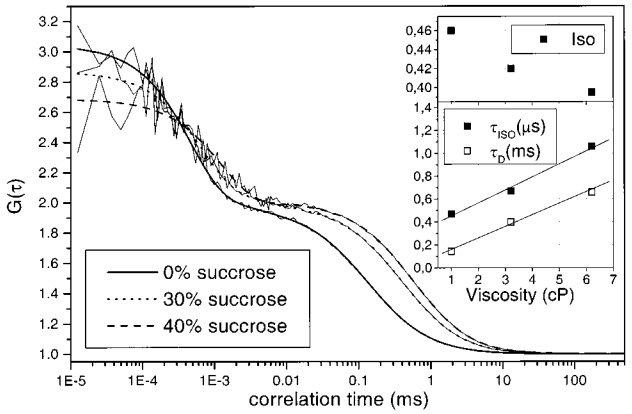

Figure 6. Effect of addition of sucrose on the isomerization properties of Cy5 in aqueous solution. At sucrose concentrations of 0, 30, and 40 wt %, corresponding to viscosities of 1, 3.2, and 6.2 Cp, the isomerization relaxation times of the FCS curves were strongly increased and the amplitudes of the process were reduced (inset). The isomerization relaxation times scaled well with the viscosity, η, and the decay time of the correlation curves due to translational diffusion, τ_D (inset).

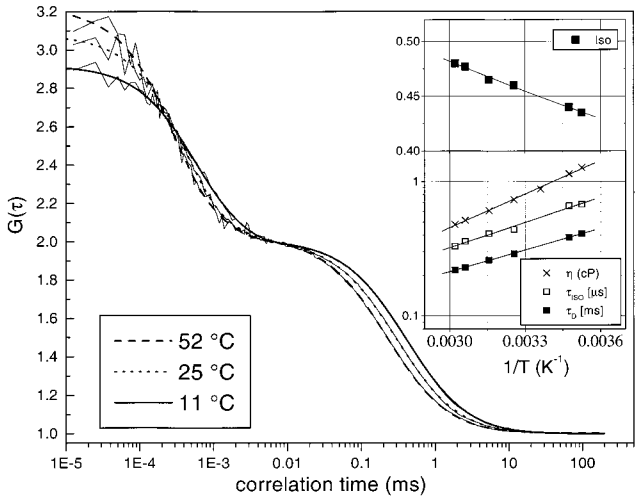

Figure 7. Temperature dependence of the isomerization kinetics of Cy5 in aqueous solution. By variation of the temperature from 11 to 55 °C a similar dependence of temperature was found as that for viscosity shown in Figure 6. The changes in the isomerization kinetics, with higher amplitudes and shorter relaxation times of the isomerization process with higher temperatures (inset), can largely be attributed to changes in viscosity induced by the temperature changes.

is well in agreement with earlier findings that, for most cyanine dyes at room temperature in alcoholic or aqueous solutions, viscosity is the dominating solvent property affecting the isomerization kinetics[31,38,48,50] and that only very small effects from changes of the polarity of the solvent are to be expected.[43,60] The lack of complete correlation between the isomerization rates and the viscosities merely reflects the complexity of the viscosity dependence and that other parameters, such as the molecular weight of the solvent molecules,[32,51] also have an impact on the isomerization rates. With increased viscosities, a decrease in the amplitudes of the isomerization relaxation process could be noted (Figure 6). This indicates that the rate of isomerization is more strongly reduced than that of the back-isomerization. For the alcohols, a somewhat lower excitation cross section was observed (Table 1), which is consistent with a red-shift of the excitation spectrum found for the Cy5 dye in alcohol solutions.[3]

The differences in the singlet−triplet transition rates are likely to reflect the different viscosities and oxygen solubilities, and to some extent polarities of these solvents, but owing to the low buildup of triplet-state molecules in some of the solvents, the relative errors of the determined triplet-state parameters are comparatively large (see Table 1).

Temperature. With increasing temperatures an increase in isomerization relaxation rates can be observed. The relative amplitudes of the isomerization process also increase, indicating that k_{ISO} increases more than σ_{BISO} (Figure 7). The relaxation times of the isomerization process, $\tau_{ISO} = 1/(k_{ISO} + k_{BISO})$, as well as the relaxation times of translational diffusion, τ_D, scale with the viscosity of the aqueous solution at the temperature at which the measurements were performed (inset, Figure 7). The dependence on temperature is similar to the viscosity dependence (inset, Figure 6), and it is therefore likely that a major part of the changes observed at different temperatures are solely due to changes in the viscosity of the solvent. The detected fluorescence emission rate per dye molecule, given by eq 27

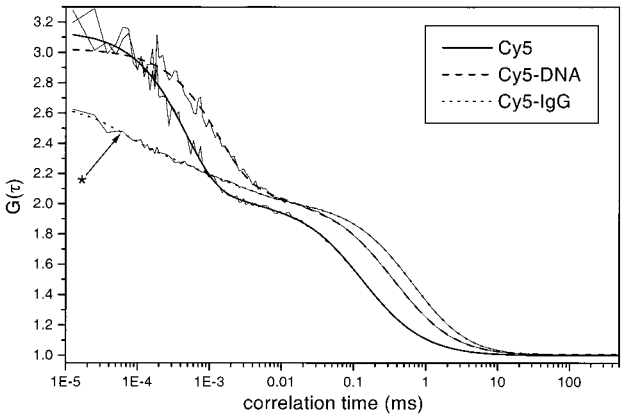

Figure 8. Effects of side groups on the isomerization properties of Cy5. Correlation curves of Cy5, Cy5−DNA (M13, double-stranded, 24 base pairs), and Cy5−IgG in aqueous solution (excitation intensity 40 kW/cm^2 at 633 nm). The addition of the DNA strand to the linker arm attached to one of the head groups of the dye leads to lower amplitudes and slower relaxation rates for the isomerization, as observed from the FCS curves. For Cy5−IgG the amplitude was very strongly reduced, which to some extent is due to multiple labeling of the IgG molecules (see text for further discussion). In the time range of 100 ns, an additional relaxation process could be observed (*), which is fully compatible with rotational diffusion.

below, increased by approximately 50% when the temperature was decreased from 52 to 11 °C.

From our data no distinct separation of the effects due to temperature or viscosity can be made. Nonetheless, the observed data are in agreement with earlier reports showing that lower temperatures lead to lower rates of isomerization and higher yields of fluorescence.[31,37,48] The lowering of the population of isomerized dyes with decreasing temperatures[40] has been attributed to the absence of an activation barrier for back-isomerization between the $^1_1$P and the $_1$Perp states.[44,60]

Effects of Side Groups. The introduction of bulky substituents on the head groups of a cyanine dye is known to generally increase the viscous drag, thereby retarding the conformational reorganizations within the molecule and reducing the rates for photoinduced isomerization and back-isomerization.[6,84] We investigated how the addition of a nucleotide (dUTP and dCTP) or a double-stranded DNA, 24 base pairs long, onto the linker arm of one of the head groups of the Cy5 influenced the fluorescence fluctuations seen via FCS. Also, Cy5-labeled immunoglobulin molecules were investigated, where the Cy5 molecules were linked to the immunoglobulins via linker chains on both their head groups (bisfunctional dye).

As expected, it was found from the FCS curves and the subsequent global analysis that both the rate of photoinduced isomerization and that of back-isomerization were retarded by substitution of a side group. The effect was more pronounced for the DNA-substituted dye than for the dyes substituted with either dCTP or dUTP (Table 1). The rates of intersystem crossing and triplet-state decay were noticeably reduced for the DNA-substituted dye. Collisional quenching of the triplet state by oxygen molecules in an air-saturated solution is for most dyes the main deactivation pathway of their triplet states, and collision by oxygen also enhances the rate of intersystem crossing. The lowered rates may therefore reflect that the dye is shielded by the DNA strand from the oxygen molecules of the aqueous solution.

The contribution of isomerization seen in the correlation curves for the Cy5-labeled IgG molecules was considerably lower than for all the other samples investigated in this study (Figure 8). From the global analysis of the correlation curves the quantum yield of photoisomerization was estimated to be about 10^{-4}, a decrease by a factor of 20 compared to that of the free dye. The effective yield of back-isomerization, on the other hand, was only decreased by a factor of 3−4. However, it should be kept in mind that the detected fluorescence rate per molecule, as given by eq 27 below, was found to be more than twice as high as that of free Cy5 dyes under similar experimental conditions. Therefore, double or even multiple labeling of fluorophores to each IgG molecule cannot be excluded. The fluctuations in fluorescence originating from each of the dyes, either due to singlet−triplet-state transitions or trans−cis isomerizations, are independent from one dye molecule to another. In a multiply labeled macromolecule the relative amplitude of the fluctuations due to photophysical phenomena will therefore decrease compared to those due to translational diffusion. In general, for a solution of freely diffusing macromolecules, where $N_m(k)$ is the mean number of molecules in the detection volume having k dye labels attached to it, the autocorrelation function, as given by eq 24, will change into

$$G(\tau) = \frac{\sum_{k=1}^{\infty} N_m(k) k^2 \left(\frac{1}{1+4D\tau/{\omega_1}^2}\right)\left(\frac{1}{1+4D\tau/{\omega_2}^2}\right)^{1/2}\left[1+\frac{1}{k}G_{fast}(\tau)\right]}{\sum_{k=1}^{\infty}(N_m(k)k)^2} + 1 \quad (25)$$

where $G_{fast}(\tau)$ is the autocorrelation function for the photophysically generated fluorescence fluctuations within one dye, as given by eq 21. Here it is assumed that all labels have the same fluorescence brightness, independent of the number of labels per macromolecule as well as of their labeling sites. While multiple labeling of the IgG molecules will lead to decreased relative amplitudes of the relaxation processes related to trans−cis isomerization and singlet−triplet interactions, the relaxation times of each of the processes will be unaffected. This means that if multiple labeling is not taken into account the rates of trans−cis isomerization and intersystem crossing will be underestimated relative to those of cis−trans back-isomerization and triplet-state decay, respectively.

From eq 24 it follows that the rate of detected photons per molecule in their singlet trans states, $k_{fl}(^1\bar{N})$, can be obtained by multiplying the amplitude of the measured AC curves with the total rate of detected photons.

$$k_{fl}(^1\bar{N}) = [\text{rate of detected photons}]G(0) = \frac{[\text{rate of detected photons}]}{N_m\,{}^1\bar{N}} \quad (26)$$

$k_{fl}(^1\bar{N})$ was found to increase by approximately 20% by substitution of a nucleotide and by approximately 50% by the substitution of the double-stranded DNA to the Cy5 dye. A significant increase of $k_{fl}(^1\bar{N})$ could also be measured in a aqueous solution of Cy5 at decreased temperatures, with a 50% enhancement of $k_{fl}(^1\bar{N})$ at 11 °C compared to that at 52 °C, as mentioned above. However, no significant change of $k_{fl}(^1\bar{N})$ could be observed as a consequence of viscosity when sucrose was added to the aqueous solution of Cy5.

$k_{fl}(^1\bar{N})$ should be independent of the isomerization properties of the Cy5 dye. On the other hand, the rate of detected photons

per molecule, irrespective of whether it is in its trans conformation or in its singlet or triplet electronic states, is given by eqs 3 and 24:

$$k_{fl} = [\text{rate of detected photons}]G_D(0) = \frac{[\text{rate of detected photons}]}{N_m} \quad (27)$$

As mentioned above, for Cy5 the fraction of isomerized molecules decreases as a consequence of substitution of a side group as well as with decreasing temperatures and viscosities. Therefore, the overall rate of fluorescence emission per molecule, k_{fl}, will for all these cases increase. It is worthwhile to point out that with a fraction of isomerized dyes close to 50%, which is generated also under relatively low CW excitation conditions, the Cy5 dye emits photons only to 50% of its capacity in the absence of trans−cis isomerization.

The correlation curves of the Cy5-labeled immunoglobulins revealed an additional exponential in the 100 ns time range, which could not be observed for the other investigated samples. This relaxation process did not change significantly with the excitation intensity and is well compatible with rotational diffusion of the Cy5-labeled IgG molecules. The presence of a contribution due to rotational diffusion in the correlation curves indicates that the dye has a restricted mobility in relation to the IgG molecule. This is well in line with the fact that the dye used for labeling was a bisfunctional dye with two linking chains at each of its headgroups.[1] The two labeling sites of the dye restrict both the ability of the dye to undergo conformational changes within the dye molecule, thereby reducing the yields of isomerization and back-isomerization, as well as the possible movement and wobbling with respect to the labeled macromolecule, so that the rotation of the dye represents the rotational mobility of the whole molecule.

Length of the Polymethine Chain. The cyanine dye Cy3 in aqueous solution, containing three carbons in the conjugated chain between the head groups instead of the five carbons of the Cy5 molecules, was excited at 515 nm with an argon-ion laser. The correlation curves showed the same behavior as those seen for Cy5 in water (data not shown). However, after global analysis of a set of correlation curves, approximately 3-fold higher isomerization and back-isomerization yields were found, in comparison to those of Cy5 (See Table 1. For an estimation of the difference in back-isomerization yields, the ratio σ_{BISO}/σ should be compared.) This is well in line with previous investigations, which state that photoinduced isomerization in general is increased with a shorter length of the conjugated hydrocarbon chain linking the two head groups of the cyanine dye.[85]

5. Concluding Remarks

Under photostationary conditions, FCS measurements not only reveal the population of the different photoinduced states but also provide time-resolved information about the states in the nanosecond to millisecond time scale. The investigations made in this study on Cy5 under various conditions indicate that the observed photophysical fluctuations in detected fluorescence, as characteristically represented in the FCS curves, can be attributed to trans−cis isomerization and transitions between the singlet and triplet states of the dye. The applied kinetic model, with the mentioned simplifications, seems to be applicable to the experimental data. Upon addition of potassium iodide the rate of intersystem crossing was increased, while no significant effects on the isomerization kinetics could be observed. With an independent experimental approach our study therefore supports the view that trans−cis isomerization takes place exclusively from the excited singlet state, without any involvement of the lowest triplet state.

In this investigation, an average excitation intensity is used to calculate the photophysical rate parameters. This simplification may in the general case introduce systematic errors. The nonuniformity of the laser excitation within the volume of detection leads to a distribution of relaxation rates for the isomerization, which cannot be successfully fitted to a monoexponential function and may also lead to over-representation of the fluorescence from the peripheral parts of the detection volume. These effects have been discussed in detail for the case of triplet-state monitoring by FCS,[70] where a more rigorous treatment is given for how to take the fluorescence intensity distribution within the sample volume into consideration. In this investigation, a narrow pinhole was used, whose projection in the focal plane of the sample is smaller than the dimensions of the excitation laser beam. This minimizes the errors introduced by the assumption of a uniform excitation. By variation of the size of the pinhole one can note that for narrow pinholes, the relaxation process in the AC curves due to isomerization can be successfully fitted to a monoexponential process. For larger pinholes, on the other hand, where the projected pinhole is about 50% bigger than the size of the laser beam in the focal plane, the nonuniformity of the laser excitation within the volume of detection becomes evident and a distribution of relaxation rates for the isomerization can be seen in the AC curves. In the absence of a pinhole the average relaxation times of isomerization, as measured in the FCS curves, were increased by approximately 25%. This reflects the additional collection of fluorescence from peripheral regions of the laser beam, where the excitation intensity is lower. The collection of fluorescence from these regions is blocked by a narrow pinhole. The overall relative amplitude of the isomerization process was not significantly influenced by the pinhole size at excitation intensities below the level of saturation.

In our model we have assumed the fluorescence capacity of the cis isomer to be negligible. For the case that the cis isomer would have a significant fluorescence quantum yield, this assumption would lead to an underestimation of the fraction of dye molecules that are in their cis forms under photostationary conditions. However, the measured relative amplitudes of the isomerization relaxation process in the FCS curves (about 0.5 for most conditions presented) indicate high relative fluctuations in fluorescence due to isomerization. A considerable contrast in the fluorescence capacity between the trans and the cis states of the dyes is required to generate relative fluctuations of this magnitude, and a fluorescence capacity of the cis conformation that exceeds 20% of that of the trans form is not compatible with an isomerization amplitude of 0.5. For a fluorescence capacity of the cis form that is below 5% of that of the trans, neglecting the cis fluorescence will lead to an underestimation of the effective isomerization rate of less than 10%, and a corresponding overestimation of the back-isomerization rate. (See ref 86 for a general discussion on the influence of quantum yields on the monitoring of kinetic processes by FCS.)

It is worthwhile to point out that owing to the low rates of thermal relaxation of the photoinduced cis state, k_{PN}, a photostationary equilibrium is established between the isomeric forms already at very modest excitation intensities, and approximately 50% of the Cy5 dye molecules will then be in their nonfluorescent or at least weakly fluorescent cis states. Cy5 has been frequently used in the last years in different applications regarding fluorescence microscopy and single-molecule detection

by fluorescence. Although the photophysical properties of the dye are of considerable importance for its performance in these applications, they are to a large extent unknown. Here we present data about triplet-state transitions and trans−cis isomerization of the Cy5 dye that have not been previously reported. Our data indicate that at photostationary equilibrium the fluorophores lose about half of their fluorescence capacity owing to population of the photoisomerized cis state. This is of relevance for the performance of the dye in all applications of fluorescence spectroscopy where a high sensitivity is required, such as in single-molecule detection experiments. Under the excitation conditions used in this study, the deactivation of the cis isomer back to the trans form almost completely takes place via excitation of the cis state. However, under lower excitation intensities thermal deactivation can be the dominating deactivation channel, leading to a different steady-state equilibrium between the isomeric forms of the Cy5 molecules. In general, if the population of nonfluorescent cis isomers is not considered, the measured fluorescence quantum yield of a cyanine dye can be strongly underestimated. It can also depend on the excitation intensity applied during the measurement, since the fraction of dyes that are in the nonfluorescent cis state may change. For the same reason, differences in the detected fluorescence upon conjugation of Cy5 dyes to proteins and DNA molecules attributed to changed fluorescence quantum yields can to some extent also be a consequence of a change in the photostationary equilibria between the isomers. For FRET measurements, where Cy5 is frequently used as an acceptor dye, the fraction of the Cy5 molecules in their cis states would still work as acceptor dye molecules, owing to the close overlap of the absorption spectra of the trans and cis isomers. The FRET efficiency to the cis state can in fact even be expected to be higher than that to the trans state, since the excitation cross section in the blue region is higher than that of the trans state. However, practically no fluorescence should be generated following energy transfer to the cis state of Cy5. Generation of cis state fluorophores can thus contribute to the absence of acceptor dye fluorescence, which was recently reported in SMD FRET measurements using Cy5 as an acceptor probe.[87] Alternatively, the resulting lower acceptor dye fluorescence would lead to an overestimation of the distance between the donor−acceptor dye pair. In general, when cyanine dyes are used to follow dynamics of single molecules, for instance, intramolecular dynamics observed via FRET, fluctuations in fluorescence induced by transitions between the trans and cis states of the dyes should be kept in mind so that they are not misinterpreted as dynamics of the labeled molecules.

For some FCS curves recorded at the highest excitation intensities in aqueous solution and in the different alcohols, the isomerization relaxation process was better fitted to a two-exponential function. From the present data it cannot be resolved whether this indicates the presence of additional isomerized states, if it is due to a somewhat nonuniform excitation within the sample volume element generating a distribution of exponential decays, if it reflects a close overlap between the relaxation times of the singlet−triplet transitions and the isomerizations within the dye (see Figure 3), or if it simply follows from the fact that an experimental curve in general can be fitted better the more parameters are introduced. We note that for some cyanine dyes, evidence has been reported for the formation of more than one isomer.[28,35,45] The question of whether additional isomers are formed for Cy5 under high excitation conditions merits further investigations.

In rotational mobility studies it is sometimes desirable that the rotation of the fluorophore represents the rotational mobility of the biological macromolecule to which it is attached. Linking both ends of the fluorescent probe to the macromolecule, as for the bisreactive Cy5 dye labeled to the IgG molecule investigated here, seems to limit the independent movement of the label, thereby fulfilling the above requirement. The possibility to measure rotational diffusion with FCS[64] has recently been shown for different mutants of the green fluorescent protein,[76] where the fluorescently active part of the protein is immobile with respect to the whole protein. The advantage with FCS is that there is no principal limitation set by the fluorescence lifetime for how slow rotations that can be measured, as is the case in fluorescence anisotropy measurements.

In the same study[76] it was shown that global analysis in combination with FCS can be used as a strategy to increase the precision in the analysis of correlation curves containing several dynamic processes, with relaxation times that cannot be sufficiently resolved when the correlation curves are analyzed individually. This strategy has also been applied in this study.

In two independent FCS investigations, different mutants of the green fluorescent protein (GFP) have revealed fluctuations in fluorescence showing a similar dependence on excitation intensity as that found for the trans−cis isomerization of Cy5. However the underlying process of these fluorescence fluctuations has still not been fully identified.[76,77] In general, it should be mentioned that FCS offers information obtained from the fluorescence fluctuations, and their time dependencies yield dynamic parameters but do not provide an absolute identification of the underlying processes. Although the FCS data would be compatible with the hypothesized processes, further investigations following the response of the dynamic parameters to various environmental conditions are often necessary, as was done in this study. Alternatively, complementary approaches, such as single-molecule detection experiments with a higher time resolution, including also spectral and time-resolved data can be used to further verify the interpretation inferred from the FCS measurements.

Nonetheless, the present study demonstrates that FCS is a useful approach to study isomerization processes between trans and cis forms of cyanine dyes and that FCS offers an attractive complementary or alternative technique to other spectroscopic techniques, such as fluorescence decay measurements and transient absorption spectroscopy, to study photophysical processes in general. In particular, to obtain information about photoinduced cis−trans back-isomerizations of cyanine dyes, a rather complicated sequence of operations is required, and the instrumentation necessary is generally more complicated than that used in FCS. In addition, for many cyanine dyes the excitation and emission spectra of the different isomers tend to overlap, making it difficult to separate them by transient absorption measurements. The concentration of dyes necessary for FCS studies is low enough to exclude any influence of dye self-aggregation or energy transfer, which has been shown to occur at concentrations above the micromolar range for cyanine dyes.[40] The low concentrations used in combination with the small sample volume element also strongly reduce the amount of material necessary for the investigations. The FCS technique is especially well adapted to investigate low quantum yield processes ($\Phi < 10^{-3}$), which cannot so easily be characterized from the very small effects on fluorescence lifetimes and the small transient absorptions that they may generate.[6,33] FCS covers a very broad time interval over which dynamic processes can be monitored, in contrast to many traditional fluorescence techniques that are restricted to a few orders of magnitude. Finally, the photophysical processes investigated here tend to be

environment sensitive and depend on the identity of the labeled molecule and the mode of labeling. Since FCS is based on a confocal fluorescence microscope, these processes can be used to locally probe a wide range of different microenvironments.

Acknowledgment. This study was supported by grants from the Magnus Bergwall Foundation, the Swedish Society of Medicine, the Swedish Foundation for International Cooperation in Research and Higher Education, the German Ministry for Education, Science, Research, and Technology, and funds from the Karolinska Institute. The authors would like to thank R. Rigler, C. Seidel, and W. W. Webb, in whose laboratories different parts of the experiments of this study were performed.

References and Notes

(1) Ernst, L. A.; Gupta, R. K.; Mujumdar, R. B.; Waggoner, A. S. *Cytometry* **1989**, *10*, 3.
(2) Mujumdar, R. B.; Ernst, L. A.; Mujumdar, S. R.; Waggoner, A. S. *Cytometry* **1989**, *10*, 11.
(3) Southwick, P. L.; Ernst, L. A.; Tauriello, E. W.; Parker, S. R.; Mujumdar, R. B.; Mujumdar, S. R.; Clever, H. A.; Waggoner, A. S. *Cytometry* **1990**, *11*, 418.
(4) Soper, S. A.; Mattingly, Q. L.; Vegunta, P. *Anal. Chem.* **1993**, *65*, 740.
(5) Sargent, P. B. *Neuroimage* **1994**, *1*, 288.
(6) Soper, S. A.; Mattingly, Q. L. *J. Am. Chem. Soc.* **1994**, *116*, 3744.
(7) Williams, D. C.; Soper, S. A. *Anal. Chem.* **1995**, *67*, 3427.
(8) Sauer, M.; Drexhage, K. H.; Zander, C.; Wolfrum, J. *Chem. Phys. Lett.* **1996**, *254*, 223.
(9) Sauer, M.; Arden-Jacob, J.; Drexhage, K. H.; Gobel, F.; Lieberwirth, U.; Muhlegger, K.; Muller, R.; Wolfrum, J.; Zander, C. *Bioimaging* **1998**, *6*, 14.
(10) Kuhn, H. *J. Chem. Phys.* **1949**, *17*, 1198.
(11) Schäfer. F. P. *Dye lasers*; Schäfer, F. P., Ed.; Springer-Verlag: Heidelberg, 1973.
(12) Lansdorp, P. M.; Smith, C.; Safford, M.; Terstappen, L. W. M. M.; Thomas, T. E. *Cytometry* **1991**, *12*, 723.
(13) Galbraith, W.; Wagner, M. C. E.; Chao, J.; Abaza, M.; Ernst, L. A.; Nederlof, M. A.; Hartsock, R. J.; Taylor, L.; Waggoner, A. S. *Cytometry* **1991**, *12*, 579.
(14) Ballard, S. G.; Ward, D. C. *J. Histochem. Cytochem.* **1993**, *41*, 1755.
(15) Schwille, P.; Meyer-Almes, F. J.; Rigler, R. *Biophys. J.* **1997**, *72*, 1878.
(16) Aubin, J. E. *J. Histochem. Cytochem.* **1979**, *27*, 36.
(17) Noonberg, S. B.; Weiss, T. L.; Garovoy, M. R.; Hunt, C. A. *Antisense Res. dev.* **1992**, *2*, 303.
(18) Ballou, B.; Fisher, G. W.; Deng, J. S.; Hakala, T. R.; Srivastava, M.; Farkas, D. L. *Cancer Detect. Prev.* **1998**, *22*, 251.
(19) Chatterjee, S.; Gattschalk, P.; Davis, P. P.; Schuster, G. B. *J. Am. Chem. Soc.* **1988**, *110*, 2326.
(20) Shank. C. V.; Ippen. E. P. *Dye lasers*; Schäfer, F. P., Ed.; Springer-Verlag: Heidelberg, 1973.
(21) Maeda. M. *Laser Dyes*; Academic Press: Tokyo, 1984.
(22) Dragsten, P. R.; Webb, W. W. *Biochemistry* **1978**, *17*, 5228.
(23) Krieg, M.; Redmond, R. W. *Photochem. Photobiol.* **1993**, *57*, 472.
(24) Benniston, A. C.; Harriman, A. *J. Chem. Soc., Faraday Trans.* **1998**, *94*, 1841.
(25) Benniston, A. C.; Harriman, A.; Mcavoy, C. *J. Chem. Soc., Faraday Trans.* **1998**, *94*, 519.
(26) Korobov, V. E.; Chibisov, A. K. *Russ. Chem. Rev.* **1983**, *52*, 27.
(27) Dempster, D. N.; Morrow, T.; Rankin, R.; Thompson, G. F. *J. Chem. Soc., Faraday Trans.* **1971**, *68*, 1479.
(28) Kuzmin, V. A.; Darmanyan, A. P. *Chem. Phys. Lett.* **1978**, *54*, 159.
(29) Chibisov, A. K. *J. Photochem.* **1977**, *6*, 199.
(30) Chibisov, A. K.; Zakharova, G. V.; Görner, H.; Sogulyaev, Y. A.; Mushkalo, I. L.; Tolmachev, A. I. *J. Phys. Chem.* **1995**, *99*, 886.
(31) Sundström, V.; Gillbro, T. *J. Phys. Chem.* **1982**, *86*, 1788.
(32) Åkesson, E.; Hakkarainen, A.; Laitinen, E.; Helenius, V.; Gillbro, T.; Korppi-Tommola, J.; Sundström, V. *J. Chem. Phys.* **1991**, *95*, 6508.
(33) He'bert, P.; Baldacchino, G.; Gustavsson, T.; Mialocq, J. C. *J. Photochem. Photobiol. A* **1994**, *84*, 45.
(34) Baraldi, I.; Carnevali, A.; Momicchioli, F.; Ponterini, G. *Spectrochim. Acta. A* **1993**, *49A*, 471.
(35) Khimenko, V.; Chibisov, A. K.; Görner, H. *J. Phys. Chem.* **1997**, *101*, 7304.
(36) Chibisov, A. K.; Zakharova, G. V.; Görner, H. *J. Chem. Soc., Faraday Trans.* **1996**, *92*, 4917.
(37) Chibisov, A. K.; Görner, H. *J. Photochem. Photobiol., A* **1997**, *105*, 261.
(38) Velsko, S. P.; Waldeck, D. H.; Fleming, G. R. *J. Chem. Phys.* **1983**, *78*, 249.
(39) Dempster, D. N.; Morrow, T.; Rankin, R.; Thompson, G. F. *Chem. Phys. Lett.* **1973**, *18*, 488.
(40) Rulliere, C. *Chem. Phys. Lett.* **1976**, *43*, 303.
(41) Redmond, R. W.; Kochevar, I. E.; Krieg, M.; Smith, G.; McGimpsey, W. G. *J. Phys. Chem.* **1997**, *101*, 2773.
(42) West, W.; Pearce, S.; Grum, F. *J. Phys. Chem.* **1967**, *71*, 1316.
(43) Ponterini, G.; Momicchioli, F. *Chem. Phys.* **1991**, *151*, 111.
(44) DiPaolo, R. E.; Scaffardi, L. B.; Duchowicz, R.; Bilmes, G. M. *J. Phys. Chem.* **1995**, *99*, 13796.
(45) Vaveliuk, P.; Scaffardi, L. B.; Duchowicz, R. *J. Phys. Chem.* **1996**, *100*, 11630.
(46) Rentsch, S.; Döpel, E.; Petrov, V. *Appl. Phys. B* **1988**, *B46*, 357.
(47) Cooper, W.; Rome, K. A. *J. Phys. Chem.* **1974**, *78*, 16.
(48) Aramendia, P. F.; Negri, R. M.; San Roma'n, E. *J. Phys. Chem.* **1994**, *98*, 3165.
(49) Noukakis, D.; Vanderauweraer, M.; Toppet, S.; Deschryver, F. C. *J. Phys. Chem.* **1995**, *99*, 11860.
(50) Velsko, S. P.; Fleming, G. R. *Chem. Phys.* **1982**, *65*, 59.
(51) Sauerwein, B.; Murphy, S.; Schuster, G. B. *J. Am. Chem. Soc.* **1992**, *114*, 7920.
(52) Arthurs, E. G.; Bradley, D. J.; Roddie, A. G. *Opt. Commun.* **1973**, *8*, 118.
(53) Aramendia, P. F.; Duchowicz, R.; Scaffardi, L.; Tocho, J. O. *J. Phys. Chem.* **1990**, *94*, 1389.
(54) Bilmes, G. M.; Tocho, J. O.; Braslavsky, S. E. *Chem. Phys. Lett.* **1987**, *134*, 335.
(55) Bilmes, G. M.; Tocho, J. O.; Braslavsky, S. E. *J. Phys. Chem.* **1988**, *92*, 5958.
(56) Zhu, X. R.; Harris, J. M. *Chem. Phys.* **1988**, *124*, 321.
(57) Ghelli, S.; Ponterini, G. *J. Mol. Struct.* **1995**, *355*, 193.
(58) Momicchioli, F.; Baraldi, I.; Ponterini, G. *Spectrochim. Acta A* **1990**, *46A*, 775.
(59) Momicchioli, F.; Baraldi, I. Berthier, G. *Chem. Phys.* **1988**, *123*, 103.
(60) Rodriguez, J.; Scherlis, D.; Estrin, D.; Aramendia, P. F.; Negri, R. M. *J. Phys. Chem.* **1997**, *101*, 6998.
(61) Magde, D.; Elson, E. L.; Webb, W. W. *Phys. Rev. Lett.* **1972**, *29*, 705.
(62) Elson, E. L.; Magde, D. *Biopolymers* **1974**, *13*, 1.
(63) Magde, D.; Elson, E. L.; Webb, W. W. *Biopolymers* **1974**, *13*, 29.
(64) Ehrenberg, M.; Rigler, R. *Chem. Phys.* **1974**, *4*, 390.
(65) Rigler. R.; Widengren. J. *Bioscience*; Klinge, B., Owman, C., Eds.; Lund University Press: Lund, Sweden, 1990.
(66) Rigler. R.; Widengren. J.; Mets. Ü. *Fluorescence Spectroscopy*; Wolfbeis, O. S., Ed.; Springer-Verlag: Berlin, 1992.
(67) Rigler, R.; Mets, Ü. *SPIE* **1992**, *1921*, 239.
(68) Mets, Ü.; Rigler, R. *J. Fluoresc.* **1994**, *4*, 259.
(69) Rigler, R.; Mets, Ü.; Widengren, J.; Kask, P. *Eur. Biophys. J.* **1993**, *22*, 169.
(70) Widengren, J.; Mets, Ü.; Rigler, R. *J. Phys. Chem.* **1995**, *99*, 13368.
(71) Chen, F. A.; Tusak, A.; Pentoney, S.; Konrad, K.; Lew, C.; Koh, E.; Sternberg, J. *J. Chromatogr.* **1993**, *652*, 355.
(72) Arago'n, S. R.; Pecora, R. *J. Chem. Phys.* **1976**, *64*, 1791.
(73) Widengren, J.; Rigler, R.; Mets, Ü. *J. Fluoresc.* **1994**, *4*, 255.
(74) Palmer, A. G.; Thompson, N. L. *Biophys. J.* **1987**, *51*, 339.
(75) Widengren, J.; Dapprich, J.; Rigler, R. *Chem. Phys.* **1997**, *216*, 417.
(76) Widengren, J.; Mets, Ü.; Rigler, R. *Chem. Phys.* **1999**, *250*, 171.
(77) Schwille, P.; Kummer, S.; Heikal, A. H.; Moerner, W. E.; Webb, W. W. *Proc. Natl. Acad. Sci. U.S.A.* **2000**, *97*, 151.
(78) Widengren, J.; Rigler, R. *Bioimaging* **1996**, *4*, 149.
(79) Eggeling, C.; Widengren, J.; Rigler, R.; Seidel, C. *Anal. Chem.* **1998**, *70*, 2651.
(80) Sauer. M. Dissertation. Heidelberg University, 1995.
(81) Sauer, M.; Angerer, B.; Han, K. T.; Zander, C. *Phys. Chem. Chem. Phys.* **1999**, *1*, 2471.
(82) Eggeling. C.; Widengren. J.; Rigler. R.; Seidel. C. A. M. *Applied fluorescence in chemistry, biology and medicine*; Rettig, W., Strehmel, B., Schrader, S., Seifert, H., Eds.; Springer-Verlag: Berlin, 1999.
(83) Drexhage. K. H. *Dye lasers*; Schäfer, F. P., Ed.; Springer-Verlag: Heidelberg, 1973.
(84) Murphy, S.; Schuster, G. B. *J. Phys. Chem.* **1995**, *99*, 8516.
(85) Graness, A.; Rentsch, S.; Werncke, W.; Tscholl, T. J.; Wigmann, H. J.; Pfeiffer, M.; Lau, A. *Teubner-Texte Phys.* **1986**, *10*, 227.
(86) Widengren, J.; Rigler, R. *Cell. Mol. Biol.* **1998**, *44*, 857.
(87) Deniz, A. D.; Dahan, M.; Grunwell, J. R.; Ha, T.; Falhaber, A. E.; Chemla, D. S.; Weiss, S.; Schultz, P. G. *Proc. Natl. Acad. Sci. U.S.A.* **1999**, *96*, 3670.